J Arid Land (2018) 10(6): 850–863
https://doi.org/10.1007/s40333-018-0075-1

Science Press Springer-Verlag

Seasonal differences in climatic controls of vegetation growth in the Beijing–Tianjin Sand Source Region of China

SHAN Lishan[1*], YU Xiang[2], SUN Lingxiao[3], HE Bin[4], WANG Haiyan[4], XIE Tingting[1]

[1] College of Forestry, Gansu Agricultural University, Lanzhou 730070, China;
[2] Chinese Academy of Forestry, Beijing 100091, China;
[3] University of Chinese Academy of Sciences, Beijing 100049, China;
[4] College of Global Change and Earth System Science, Beijing Normal University, Beijing 100875, China

Abstract: Launched in 2002, the Beiing–Tianjin Sand Source Control Project (BTSSCP) is an ecological restoration project intended to prevent desertification in China. Evidence from multiple sources has confirmed increases in vegetation growth in the BTSSCP region since the initiation of this project. Precipitation and essential climate variable-soil moisture (ECV-SM) conditions are typically considered to be the main drivers of vegetation growth in this region. Although many studies have investigated the inter-annual variations of vegetation growth, few concerns have been focused on the annual and seasonal variations of vegetation growth and their climatic drivers, which are crucial for understanding the relationships among the climate, vegetation, and human activities at the regional scale. Based on the normalized difference vegetation index (NDVI) derived from MODIS and the corresponding climatic data, we explored the responses of vegetation growth to climatic factors at annual and seasonal scales in the BTSSCP region during the period 2000–2014. Over the study region as a whole, NDVI generally increased from 2000 to 2014, at a rate of 0.002/a. Vegetation growth is stimulated mainly by the elevated temperature in spring, whereas precipitation is the leading driver of summer greening. In autumn, positive effects of both temperature and precipitation on vegetation growth were observed. The warming in spring promotes vegetation growth but reduces ECV-SM. Summer greening has a strong cooling effect on land surface temperature. These results indicate that the ecological and environmental consequences of ecological restoration projects should be comprehensively evaluated.

Keywords: vegetation growth; climatic drivers; seasonal variation; ecological engineering; interaction; Beiing–Tianjin Sand Source Controlling Project (BTSSCP); NDVI

Citation: SHAN Lishan, YU Xiang, SUN Lingxiao, HE Bin, WANG Haiyan, XIE Tingting. 2018. Seasonal differences in climatic controls of vegetation growth in the Beijing–Tianjin Sand Source Region of China. Journal of Arid Land, 10(6): 850–863. https://doi.org/10.1007/s40333-018-0075-1

1 Introduction

Since the 1970s, the Chinese government has carried out a series of engineering projects to prevent environmental and ecological degradation (Cao, 2011; Cao et al., 2011). The Beijing–Tianjin Sand Source Control Project (BTSSCP), one of the most important of restoration projects (Wu et al., 2014), was launched in 2002 to combat desertification and reduce sandstorms

*Corresponding author: SHAN Lishan (E-mail: shanls@gsau.edu.cn)
Received 2018-05-20; revised 2018-09-25; accepted 2018-10-03

around Beijing. The first phrase of this project was completed in 2010, and its environmental and ecological effects have raised great awareness from the government and scientific community.

Previous studies have extensively assessed changes in climate (Shan et al., 2015), soil properties (Zeng et al., 2014), sandstorm frequency (Qin et al., 2012), ecosystems (Liu et al., 2013; Tian et al., 2015), land degradation (Zhang et al., 2012), etc. throughout the BTSSCP region. Vegetation condition is a main indicator for reflecting the effects of ecological restoration (Liu et al., 2013; Wu et al., 2014). Investigations based on *in situ* observations and remote sensing monitoring have reported increased vegetation activity and reduced desertification since the launch of the BTSSCP (Liu et al., 2013; Wu et al., 2013). For example, based on the normalized difference vegetation index (NDVI) and indicators of desertification, Li et al. (2015) found that the ecological conditions were improved over approximately half of the BTSSCP region from 2000 to 2010. According to the vegetative state indicated by NDVI, Zhang et al. (2012) evaluated the influence of ecological restoration on sand dunes in a prominent sandstorm region, Horqin Sand Land, China. Their results showed that during the period from 1999 to 2007, 76% of the study region experienced ecological improvements, indicating the effectiveness of ecological engineering projects. Despite the usefulness of these studies on the BTSSCP region, the majority have only assessed relative short-term change in vegetation, whereas few have focused on seasonal differences in vegetation change.

In addition, it is generally agreed that precipitation and soil moisture conditions dominate vegetation growth in the BTSSCP region (Liu et al., 2013; Wu et al., 2013; Li et al., 2015). This appears reasonable because the majority of this region is characterized by an arid climate. However, as few studies have focused on seasonal variations in vegetation growth in this region, it is unclear whether precipitation is always the main constraint of vegetation growth at the seasonal scale. A recent study conducted in the arid Sahel region of Africa suggested that climate factors, such as temperature and humidity, may influence the response of vegetation to precipitation in arid environments (Rishmawi et al., 2016). In addition, the increasing trend of growing season temperature over North China is decelerating, and this deceleration has decreased reference evapotranspiration (ET) over the northern BTSSCP region (Shan et al., 2015; He et al., 2017). However, how temperature changes will impact regional vegetation activities is still poorly understood. There are still uncertainties about the drivers of vegetation change in the BTSSCP region. Re-examining the climatic drivers of vegetation growth in the BTSSCP region is crucial for ecosystem management and future environmental planning in this region.

The goals of this study were to monitor vegetation growth in the BTSSCP region with a highlight on seasonal variations, and to explore the effects of climatic drivers on vegetation growth. In addition to conventional meteorological data, remote-sensing soil moisture and drought index data were used to support our analysis.

2 Data and methods

2.1 Study area

The BTSSCP region (38°50′–46°40′N, 109°30′–119°20′E), located in the north of China, includes Beijing, Tianjin, the northern parts of Hebei and Shanxi provinces, the central part of Inner Mongolia and a small part of Shanxi Province (Shan et al., 2015). Specifically, the region is bounded by Darhan Muminggan Joint Banner of Inner Mongolia on the west, Pingyuan County of Hebei Province on the east, Daixian County of Shanxi Province on the south, and East Ujimqin Banner of Inner Mongolia on the north (Wu et al., 2012). The total area of the BTSSCP region is 4.6×10^5 km^2. Desertified land covered an area of 101.2 km^2 before the initiation of the BTSSCP. More than 80% of the BTSSCP region is covered by grassland (Fig. 1), which is home to 19.6×10^6 residents who mainly subsist on animal husbandry and agriculture. This region is dominated by a temperate continental monsoon climate with hot-wet summers and cold-dry winters. Annual mean temperature ranges from 0.6°C to 12.0°C in this region (Liu et al., 2013). Precipitation exhibits large spatial variations, ranging from more than 600 mm in the southeast to

less than 150 mm in the northwest (Liu et al., 2013). The annual total precipitation is much lower than the potential ET, producing prevailing arid and semi-arid climate conditions.

The arid and semi-arid environments and strong north winds resulting from high atmospheric pressure in Mongolia contribute to sandstorms during winter and spring. Since 2001, several measures have been employed to combat desertification, including grassland fencing, afforestation, and grazing management (prohibition, rest, or rotation). With the recovery of vegetation conditions over the past decade, the occurrence of sandstorms has decreased significantly (Wu et al., 2012).

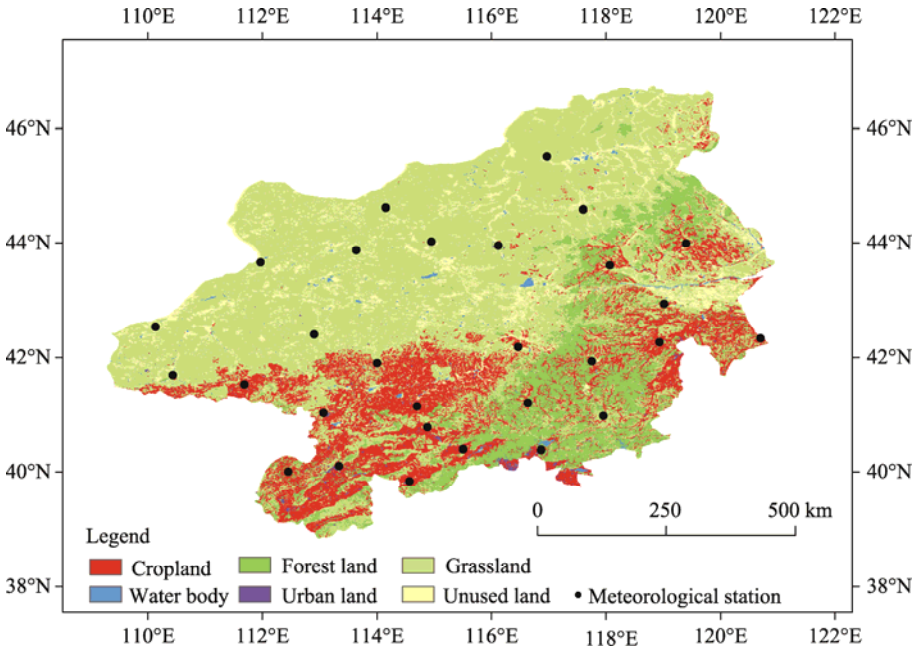

Fig. 1 Land use types and location of 28 meteorological stations (used in this study) in the Beijing–Tianjin Sand Source Control Project (BTSSCP) region

2.2 Data collection

Table 1 lists all datasets used in this study. The NDVI acquired from the MODIS (Moderate Resolution Imaging Spectroradiometer) was used to represent vegetation growth conditions. This MODIS NDVI product (MOD13A2) has a 16-d temporal resolution and a 1-km spatial resolution. The 16-d NDVI data were averaged into monthly, seasonal, and annual values over the period of 2000–2014.

Climatic data (including temperature and precipitation) in the BTSSCP region during the period from 2000 to 2014 were collected from the National Meteorological Information Center of China Meteorological Administration (http://data.cma.cn). It should be noted that the data accuracy was examined with error analysis before being issued. According to the data description (http://data.cma.cn/data/cdcdetail/dataCode/SURF_CLI_CHN_MUL_DAY_V3.0.html), the data have been checked repeatedly to correct errors through manual verification, and the missing data have been supplemented. To match the spatial resolution of MODIS data, we interpolated daily temperature and precipitation data from 28 stations into 1 km resolution using the thin plate spline interpolation method (Hutchinson, 1995).

To support our analysis, we used drought index, ET and soil moisture data to indicate moisture conditions over the study region. The standardized precipitation evapotranspiration index (SPEI), which is defined on the basis of surface water balance theory (Vicenteserrano et al., 2010), was used to represent soil moisture in this study. Monthly and seasonal SPEI data for the study region were extracted from the SPEIbase v.2.4 product (http://digital.csic.es/handle/10261/128892). This product provides multi-timescale global SPEI data with a spatial resolution of 0.5° (Beguería et

al., 2010, 2014). In this study, SPEI with a 3-month temporal resolution was used because it has been suggested to a better representation of soil moisture than SPEI with other timescales. The 8-d, 1-km ET product (MOD16A2) used in this study was estimated using the Penman-Monteith equation and MODIS retrievals (Mu et al., 2011). The accuracy of this product is considered as reasonable (Batra et al., 2006; Velpuri et al., 2013). The essential climate variable-soil moisture (ECV-SM) product was obtained from the European Space Agency (ESA) (Dorigo et al., 2012), which provides daily global soil moisture observations with a spatial resolution of 0.5°. We merged soil moisture retrievals from four passive and two active microwave sensors to obtain this product (Liu et al., 2011). Evaluations of ECV-SM product have shown that it is comparable to other soil moisture products and can capture precipitation trends (Dorigo et al., 2012).

To explore the change of land water condition in the study region, we extracted monthly total water storage (TWS) from April 2002 to November 2014 in the study region from the global land water storage retrieved from the satellite Gravity Recovery and Climate Experiment (GRACE) (Swenson and Wahr, 2006). This product provides accurate TWS estimates, and has been widely used in assessments of TWS variation at regional and global scales (Tang et al., 2013). To explore inter-annual variation in TWS, we removed seasonal TWS signals by subtracting the monthly series from the corresponding monthly climatological means (Yang et al., 2015).

The main land use types with a spatial resolution of 1 km in the study region (Fig. 1) were determined from the China's Land-Use/cover Datasets (CLUDs) obtained from the Resources and Environment Data Center, Chinese Academy of Sciences, China (Liu et al., 2014). The digital map of 2005 was used, as shown in Figure 1.

Table 1 Datasets used in this study

Variable	Product	Temporal resolution	Spatial resolution	Period
NDVI	MOD13A2	16-d	1-km	2000–2014
Temperature	-	Monthly	Whole study region	2000–2014
Precipitation	-	Monthly	Whole study region	2000–2014
Soil moisture	ECV-SM	Daily	0.5°	2000–2014
SPEI	SPEIbase v.2.4	Monthly	0.5°	2000–2014
ET	MOD16A2	8-d	1-km	2000–2014
TWS	GRACE Tellus	Monthly	1.0°	Apr 2002–Dec 2014
Land use map	China's Land-Use/cover Datasets		1-km	2005

Note: NDVI, normalized difference vegetation index; SPEI, standardized precipitation evapotranspiration index; ET, evapotranspiration; TWS, total water storage; ECV-SM, essential climate variable-soil moisture; GRACE, Gravity Recovery and Climate Experiment. "-" means that temperature and precipitation data were derived from the http://data.cma.cn.

2.3 Methods and data analysis

Changes in NDVI were investigated over four seasons: March to May (MAM; spring), June to August (JJA; summer), September to November (SON; autumn), and December to February (DJF; winter). It is noted that we excluded winter in the following analysis due to weak vegetation activity in this season. We averaged the 16-d NDVI values for each season to obtain the seasonal mean. Similarly, we determined the seasonal means of all other variables used in this study.

Seasonal and inter-annual linear trends of NDVI and climatic factors over the period of 2000–2014 were determined using the Mann-Kendall (MK) test. This nonparametric method does not need the normal distribution of time series and was recommended for general use by the World Meteorological Organization (Mitchell et al., 1966). To explore the differences in trends among different biomes, we classified the vegetation over the whole study region into three main types, including forests, grasses, and crops. Their corresponding trends over the study period were also determined. Pearson's correlation analysis was employed to examine relationships between NDVI and corresponding climatic variables including temperature, precipitation, ECV-SM and

SPEI. Correlations and trends were considered statistically significant at $P<0.05$ level. Above data analysis was performed using MATLAB software, and figures used in this study were drawn using MATLAB software and GIS software.

3 Results

3.1 Improved vegetation growth in the BTSSCP region

During the study period from 2000 to 2014, vegetation growth in the BTSSCP region improved at both annual and seasonal scales (Figs. 2 and 3). Significant increases in vegetation growth were observed over 26.4% of the study region, mainly in the southern and southeastern parts (Fig. 2a). However, significant decreases in vegetation growth only accounted for 0.8% of the study region, which were scattered over the central part. At the biome scale, a significant increase in NDVI was observed for all main vegetation types (Figs. 2b1–b3). Forests experienced the largest increase in NDVI, followed by crops and grasses. Over the study region as a whole, NDVI generally increased from 2000 to 2014, at a rate of 0.002/a (Fig. 2b4). Relatively low NDVI values in 2001, 2007, and 2009 could be attributed to drought disturbances.

Increased vegetation activity was also apparent at seasonal scales (Fig. 3), with significant increases in summer, during which significant positive trends were found over more than 30.0% of the study region (Fig. 3a). Large increases in NDVI also occurred in spring, covering 28.0% of the study region (Fig. 3b). However, relatively large decreases in NDVI were observed in autumn, accounting for 1.9% of the study region (the northern and central parts; Fig. 3c). Seasonal differences in NDVI changes were also apparent for different vegetation types (Figs. 3d1–f4). For crops, the largest NDVI increase was found in spring, followed by summer and autumn. The NDVI of grasses and forests both experienced the largest increase in summer and the smallest increase in autumn. The largest increase of the integrate NDVI within the whole study region occurred in summer (with a rate of 0.0016/a), followed by spring (0.0012/a) and autumn (0.0004/a).

3.2 Relationships between annual vegetation growth and climatic variables

Figure 4 shows the spatial patterns of correlations between annual NDVI and corresponding climatic variables over the period from 2000 to 2014. Positive relationships between annual NDVI and precipitation were observed over almost the entire study region (Fig. 4a), especially in the western and northern parts, indicating the dominant influence of precipitation on annual vegetation growth. Significant positive annual NDVI-precipitation relationships were found over about 47.6% of the study region. The dominant role of precipitation in controlling vegetation growth has been documented in previous studies (Liu et al., 2013; Wu et al., 2013), and was supported here by strong positive relationships between annual NDVI and ECV-SM and between annual NDVI and SPEI (Figs. 4c and d). In contrast, weak relationships between annual NDVI and temperature were observed (Fig. 4b), with positive relationships in the southeastern part and negative relationships in the northwestern part of the study region. Significant relationships were found over only 2.0% of the study region. The above analysis suggests that inter-annual variation in vegetation growth in this region is mainly driven by precipitation.

3.3 Relationships between seasonal vegetation growth and climatic variables

Relationships of NDVI with precipitation and temperature at seasonal scales were also investigated. As shown in Figures 5a1–a3, the relationships between seasonal NDVI and precipitation varied seasonally. Positive relationships were observed during all three seasons (spring, summer and autumn), with correlations significant in summer, followed by autumn. In spring, significant relationships were found only over small areas in the eastern and western parts, suggesting strong influences of other factors on vegetation growth. Figures 5b1–b3 show the NDVI-temperature relationships in spring, summer, and autumn, respectively. An apparent shift in NDVI-temperature relationships was observed between spring and summer. Specifically, NDVI positively responded to temperature changes in spring, whereas a significant negative relationship

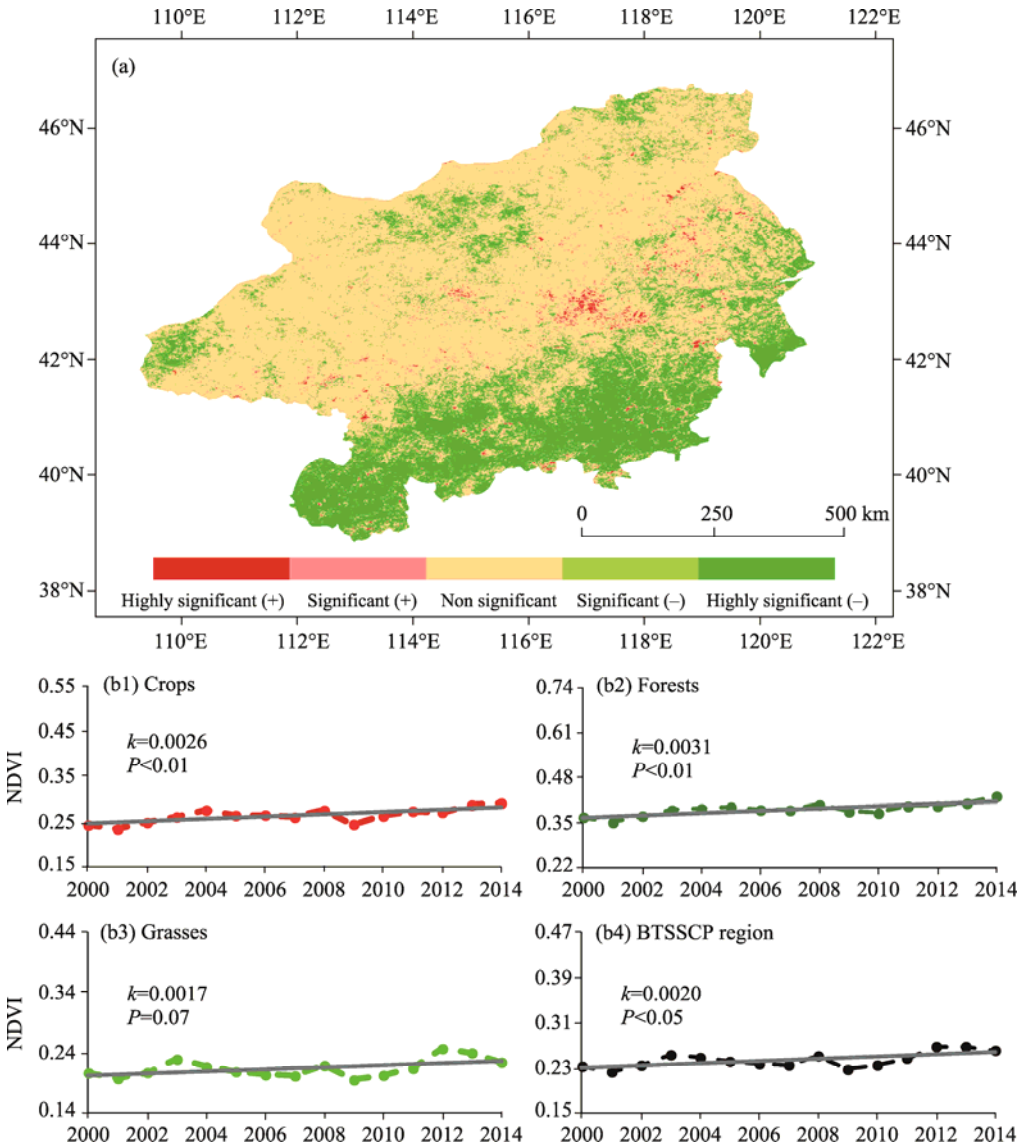

Fig. 2 Variation of NDVI trends in the BTSSCP region from 2000 to 2014. (a), spatial variation of NDVI trends; (b1), linear trend of NDVI for crops; (b2), linear trend of NDVI for forests; (b3), linear trend of NDVI for grasses; (b4), linear trend of NDVI for the study region as a whole (BTSSCP region).

was observed between NDVI and temperature in summer. In autumn, a weak positive relationship was observed over the majority of the study region. Correlation coefficients between seasonal NDVI and temperature and between seasonal NDVI and precipitation were also calculated for the whole study region. The results are basically consistent with above spatial analysis. In spring, a significant positive relationship was observed between NDVI and temperature (r=0.5543, P<0.05), while it was converted to a significant negative relationship (r= –0.7080, P<0.05) in summer. In contrast, the positive correlation between NDVI and precipitation was very weak (r=0.0809, P=0.7744) in spring, while this positive relationship was greatly improved in summer (r=0.6324, P<0.05). In autumn, there was no significant relationship between NDVI and precipitation (r=0.2541, P=0.3786) or between NDVI and temperature (r=0.0029, P=0.9919). Therefore, we speculate that temperature has a stronger effect on vegetation growth than precipitation in spring, whereas precipitation controls vegetation growth in summer. In autumn, precipitation appears to have a stronger impact on vegetation growth than temperature. The above analysis suggests that climatic constraints of vegetation growth have large seasonal differences.

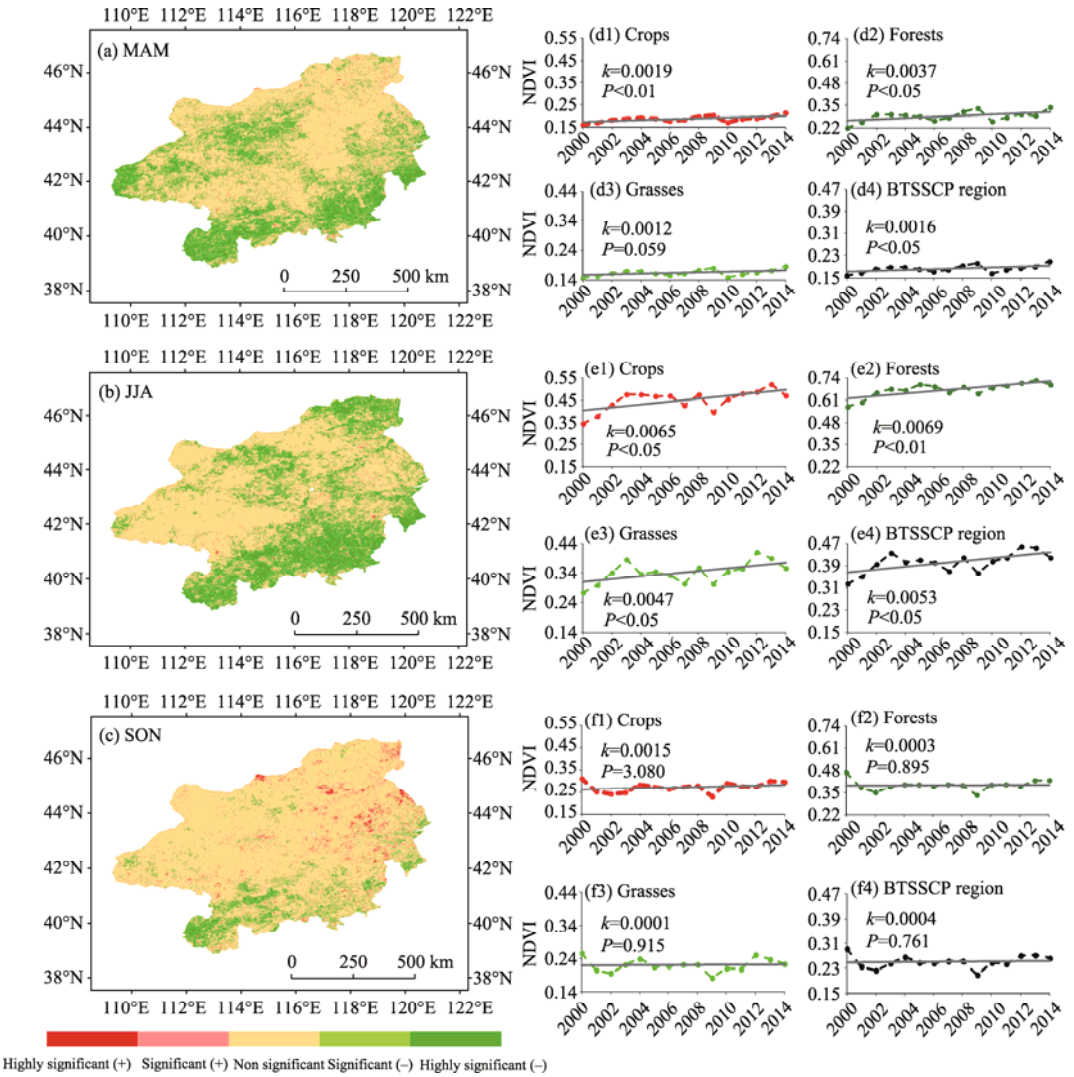

Fig. 3 Seasonal variation of NDVI trends in the BTSSCP region from 2000 to 2014. (a)–(c), spatial variations of NDVI trends for spring (March to May (MAM)), summer (June to August (JJA)) and autumn (September to November (SON)), respectively; (d)–(f), linear trends of NDVI for different vegetation types (crops, forests and grasses) and for the whole study region in spring (d1–d4), summer (e1–e4) and autumn (f1–f4), respectively.

To confirm the above findings, we further examined the relationships of NDVI with ECV-SM and SPEI (Fig. 6). We estimated these two indicators based on completely different data sources. The distributions of NDVI-ECV-SM and NDVI-SPEI correlations displayed similar patterns at seasonal scales. The impact of ECV-SM on vegetation growth was strongest in summer, which was consistent with the pattern of NDVI-precipitation relationships. In spring, NDVI showed weak positive or negative relationships with ECV-SM and SPEI, further supporting the finding that precipitation and related ECV-SM do not drive vegetation growth during this season. In autumn, NDVI positively and weakly correlated with ECV-SM and SPEI, suggesting the influences of other factors on vegetation growth in this season.

4 Discussion

In this study, we examined vegetation growth in the BTSSCP region during 2000–2014 at both annual and seasonal scales. The overall increasing trend of vegetation growth observed throughout the study region illustrates the success of restoration management, which is consistent

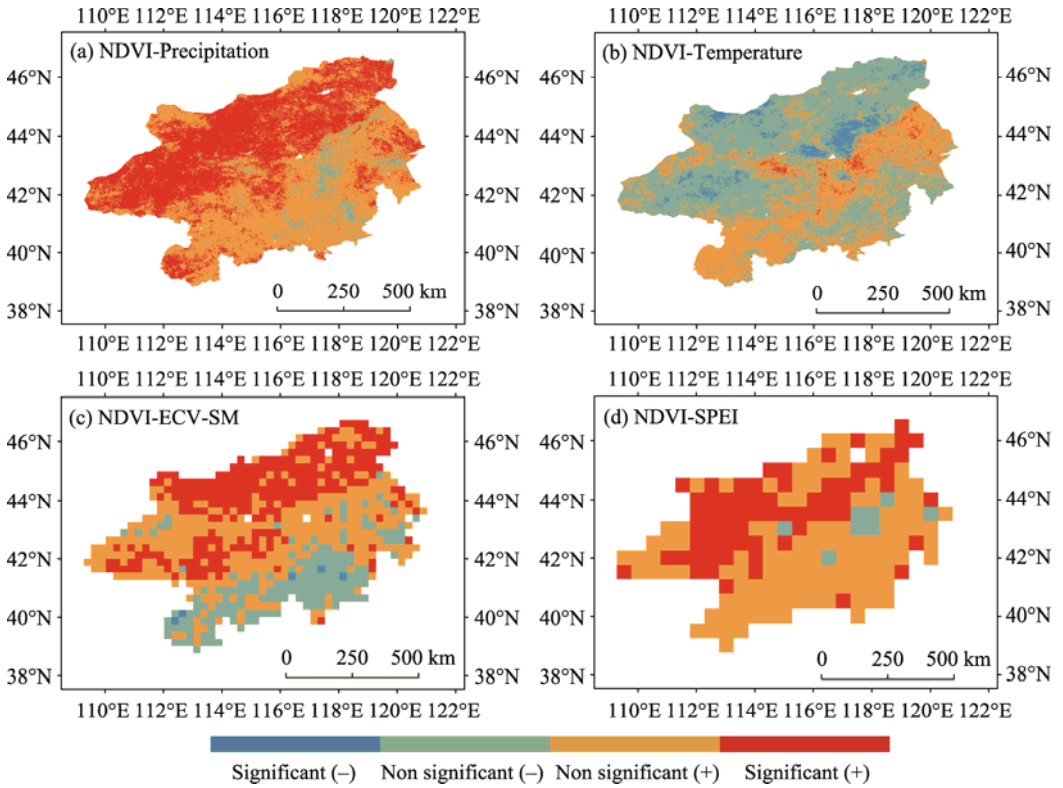

Fig. 4 Spatial patterns of the relationships of annual NDVI with (a) precipitation, (b) temperature, (c) ECV-SM, and (d) SPEI in the BTSSCP region from 2000 to 2014. ECV-SM, essential climate variable-soil moisture; SPEI, standardized precipitation evapotranspiration index. Relationships are not shown in areas with missing values in the datasets.

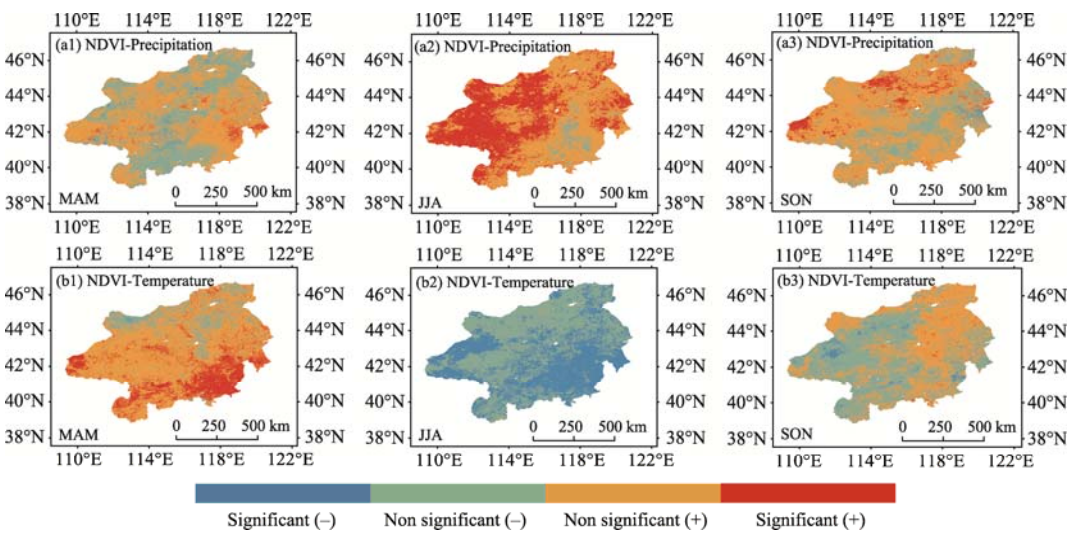

Fig. 5 Spatial patterns of the relationships of seasonal NDVI with (a1–a3) precipitation and (b1–b3) temperature in spring (a1, b1), summer (a2, b2) and autumn (a3, b3) in the BTSSCP region from 2000 to 2014. Relationships are not shown in areas with missing values in the datasets.

with previous investigations. Wu et al. (2013) reported improved vegetation conditions during 2000–2010 in the BTSSCP region based on MODIS NDVI data. In comparison, we observed larger and more extensive increases in vegetation growth during 2000–2014 based on a longer

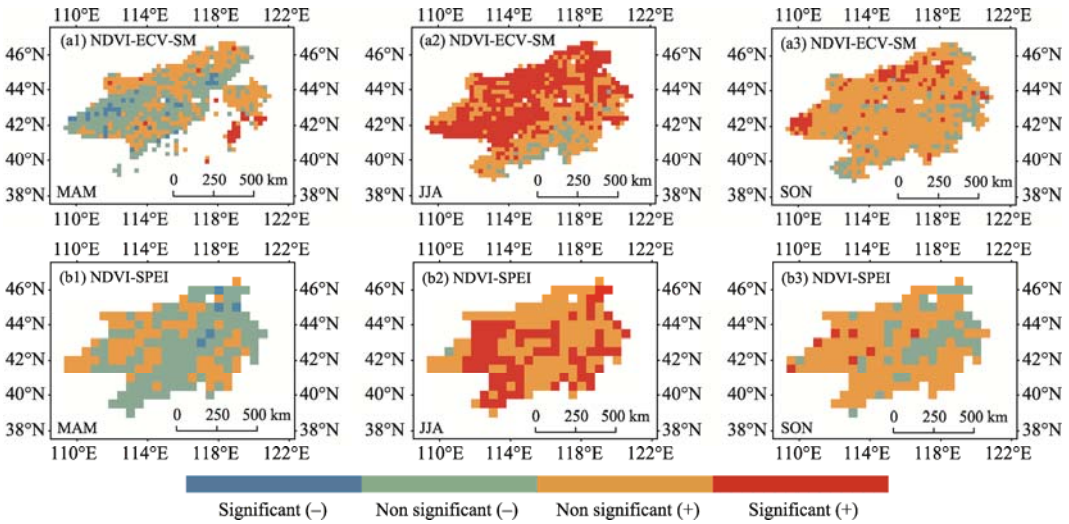

Fig. 6 Spatial patterns of the relationships of seasonal NDVI with (a1–a3) ECV-SM and (b1–b3) SPEI in spring (a1, b1), summer (a2, b2) and autumn (a3, b3) in the BTSSCP region from 2000 to 2014. Relationships are not shown in areas with missing values in the datasets.

NDVI time series. Although human activities such as afforestation, enclosure, etc. contribute to the improved vegetation growth, sustained vegetation growth relies more on climatic conditions (Wu et al., 2013). Traditionally, precipitation is thought to be the main climatic constraint of vegetation growth in this region. Liu et al. (2013) studied NDVI-precipitation relationships in the BTSSCP region during the period 1982–2006, and found a significant relationship between peak NDVI and 1-month cumulative precipitation. However, our study claimed a shift in climatic controls on vegetation growth between seasons. We analyzed the spatial variations of climatic factors (precipitation, temperature, ECV-SM, SPEI and ET) as well as TWS retrieved from GRACE during different seasons from 2000 to 2014 (Fig. 7) to explore the mechanisms of climatic drivers on vegetation growth in the BTSSCP region.

4.1 Influences of warming in spring on vegetation growth and soil moisture

As mentioned above, temperature appears to have a stronger influence on vegetation growth than precipitation in spring. This finding can be partly supported by Mohammat et al. (2013), who had also claimed a dominant influence of temperature on vegetation growth in spring in Inner Asia. In spring, precipitation significantly increased over the eastern part of the study region, whereas a strong warming was observed in the western and southwestern parts (Figs. 7a1–b3). According to previous studies (Peng et al., 2011; Xu et al., 2013), we speculate that strong warming in spring stimulates vegetation growth by triggering early onset of the growing season and promoting high photosynthetic rates. National-scale phenological investigations have suggested that warming in spring has caused an overall earlier onset of the growing season in China over the past several decades (Ma and Zhou, 2012; Ge et al., 2015). In a study of phenological variations in the Mongolian Plain, Miao et al. (2013) reported an "earlier spring" during the period 1982–2012. An examination of phenological dynamics in grasslands of Inner Mongolia using MODIS NDVI series suggested that the start of the growing season occurred 2.43 to 5.79 days earlier over the period 2002–2014 (Gong et al., 2015). In addition, an earlier investigation in eastern Central Asia suggested that both early and late green-up occurred in the Mongolian steppes during 1982–1990, and the pattern of plant response to warming was determined by the water availability conditions (Yu et al., 2003). In this study, the improved vegetation growth was also reflected by variations in ECV-SM in spring. As shown in Figure 7c1, the ECV-SM significantly decreased over the western and southwestern parts of the study region due to strong warming associated with improved vegetation growth. Similar phenomenon has also been observed during the spring of 2012 in the United State that warming in spring aggravated soil water limitation (Wolf et al., 2016).

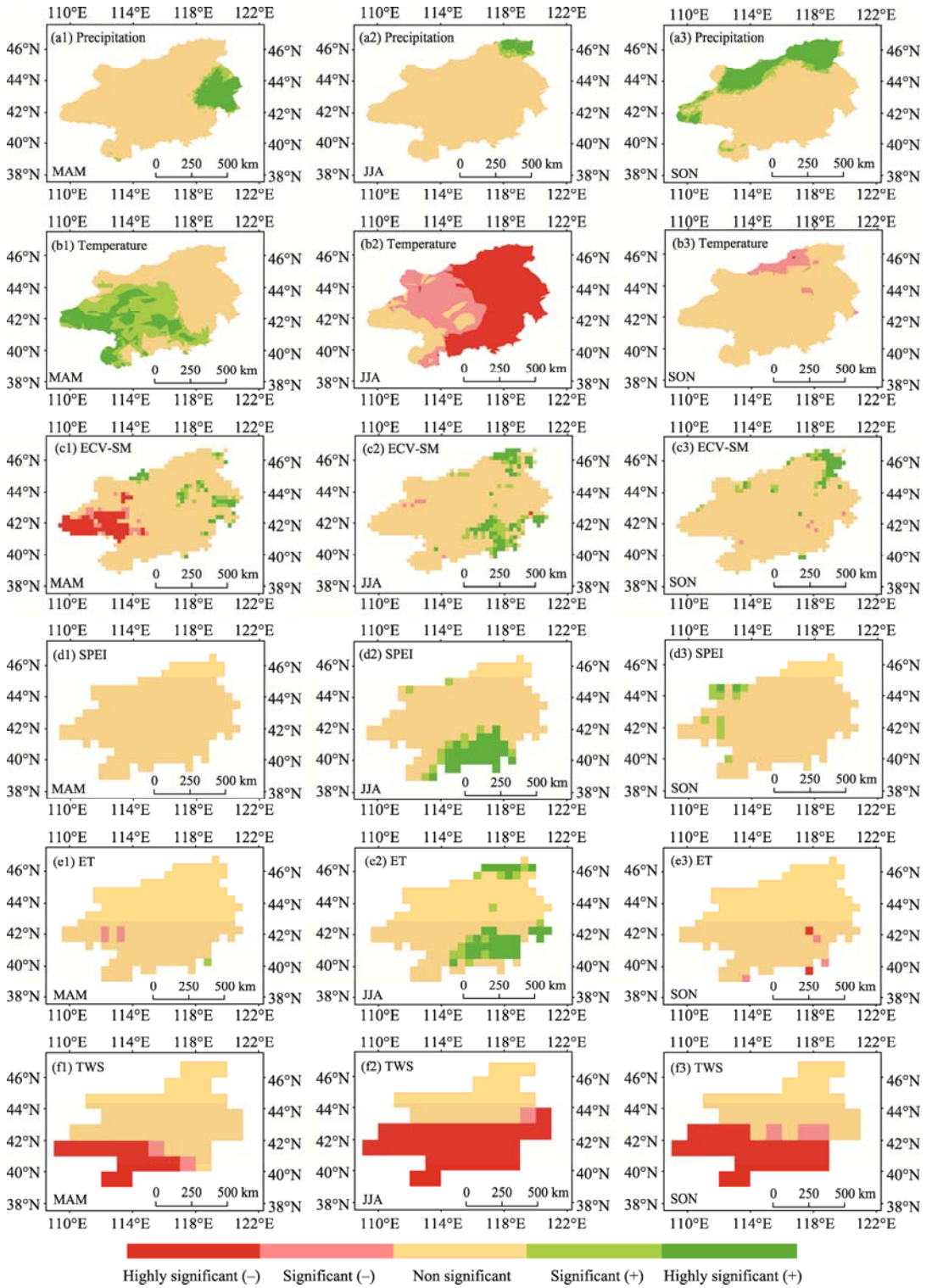

Fig. 7 Spatial patterns of trends in (a1–a3) precipitation, (b1–b3) temperature, (c1–c3) ECV-SM, (d1–d3) SPEI, (e1–e3) ET, and (f1–f3) TWS for different seasons from 2000 to 2014. ET, evapotranspiration; TWS, total water storage. Trends are not shown in areas with missing values in the datasets.

4.2 Influences of summer greening on land surface temperature

In this study, we found a dominant impact of precipitation on vegetation growth in summer.

Significantly increased precipitation was observed during 2000–2014 in small areas of the northeastern study region (Fig. 7a2), whereas more apparent increases in ECV-SM occurred in the northeastern and southeastern parts (Fig. 7c2). Increased ECV-SM promoted vegetation growth during this season. From spring to summer, the NDVI-temperature relationships changed from positive to negative and significant decreases in temperature occurred over the eastern part of the study region in summer (Fig. 7b2). We speculate that the temperature decreases were an effect of greening-associated cooling. Jiang et al. (2015) comprehensively analyzed the relationship between vegetation change and local surface temperature in northern China over the past three decades, and found a significant negative impact of vegetation change on air temperature. Similarly, Shen et al. (2015) observed a strong evaporative cooling caused by vegetation growth in the Tibetan Plateau of China. In addition, afforestation in China was found to have a cooling effect on local temperature (Peng et al., 2014). Recently, a global investigation suggested that the increase in leaf area index could generate an evaporation-driven cooling effect in arid regions (Forzieri et al., 2017). Vegetation can influence temperature through two opposite biophysical mechanisms according to previous knowledge. Elevated ET due to improved vegetation growth produces a cooling effect by consuming land surface sensible heat (Li et al., 2015). Simultaneously, the reduced albedo allows more energy to be absorbed by the land surface, thereby causing a warming effect (Li et al., 2015). The balance between these two opposite energy processes determines the ultimate change in temperature (Peng et al., 2014). Confined to the results of this study, the stronger cooling effect of greening in summer compared with the warming effect in spring produced a net cooling of land surface temperature at the regional scale. This is supported by significant increases in ET over the northern and southern parts of the study region (Fig. 7e2).

4.3 Complex attributes of autumn vegetation growth

In autumn, vegetation growth appears to be driven by both temperature and precipitation in the study region. Significant wetting trends and non-apparent cooling trends occurred in the northern part of the study region (Figs. 7a3 and b3), but there was no apparent change in temperature or precipitation in other areas. The significant decreases in vegetation growth scattered in the northeastern part may not be attributed to climatic factors. In contrast with the land use map shown in Figure 1, the decreased vegetation growth was mainly concentrated in cropland and grassland, indicating a large influence of agricultural and livestock production activities on vegetation change. According to previous reports (Hu et al., 2008; Bao et al., 2009), this decrease could be attributed to the mowing of grasses, which usually begins in late August or early September in each year. The meadow grassland is mainly utilized as the mowing pasture at a frequency of once a year (Liu et al., 2010).

4.4 Potential influence of greening on land water storage

A major concern about ecological engineering project in this arid and semi-arid region is its potential impact on water storage. Cao et al. (2011) has pointed out that afforestation in arid and semi-arid regions may dry out surface soil water and further deplete deep soil water. Feng et al. (2016) reported that new planting in the semi-arid Loess Plateau of China increases ET and that extensive vegetation expansion may influence the water demand of socio-economic systems. Based on TWS retrieved from GRACE (Figs. 7f1–f3), we observed a strong decrease in TWS in the southern part of the study region in all three seasons (spring, summer and autumn); however, there was no apparent decrease in precipitation in these areas (Figs. 7a1–a3). Areas with decreased TWS were corresponded with greening areas (Fig. 3). This coincidence raises the conjecture that greening in summer contributes to the decrease of TWS in these areas, as further supported by the increase in ET in the southern part of the study region in summer (Fig. 7e2). In contrast with land use map (Fig. 1), the decreased TWS was mainly concentrated in cropland, indicating a strong influence of agricultural activities on regional greening and thereby the depletion of land water storage. Tang et al. (2013) investigated the TWS changes in North China and found that the depletion of TWS can mainly be attributed to anthropogenic impacts,

especially the agricultural irrigation. It is still not clear that whether the greening caused by ecological engineering has contributed to the decrease of TWS. Therefore, further clarification of the influences of environmental changes and human activities on TWS is needed to address this issue.

5 Conclusions

The effectiveness of the BTSSCP, a huge ecological engineering project, has caused great public and scientific awareness. This study comprehensively analyzed vegetation conditions and their climatic drivers in the BTSSCP region from 2000 to 2014 at both annual and seasonal scales. An overall increase in vegetation growth was observed, with most significant increases occurring in spring and summer. Climatic drivers of vegetation growth varied seasonally. Temperature and precipitation mainly stimulate vegetation growth in spring and summer, respectively. The warming in spring promotes vegetation growth while reduces ECV-SM. Summer greening has a large cooling effect on land surface temperature. The co-occurrence of greening and decreased TWS in the southern part of the study region indicates the potential influence of improved vegetation growth on the depletion of TWS. Based on the results of this study, we infer that the drivers of vegetation growth in the BTSSCP region may be more complex than originally thought and that the traditional precipitation-based projections of vegetation growth in this region may be misleading. In addition, we clarified some of the ecological and environmental consequences of greening, which typically have been ignored in previous researches. Future investigations should pay more attention to these issues. This study provides important information for the design of ecological engineering projects in this region in the future.

Acknowledgements

This work was financially supported by the National Natural Science Foundation of China (31560135, 41361100), the Discipline Construction Fund Project of Gansu Agricultural University (GAU-XKJS-2018-104, GAU-XKJS-2018-108) and the Gansu Science and Technology Support Program (1604FKCA088). The authors are very grateful to the anonymous reviewers and editors for their critical review and comments which helped to improve and clarify the manuscript.

References

Bao A Y, Bao G, Guo L, et al. 2009. Evaluation on vegetation net primary productivity using MODIS data in Inner Mongolia. Proceedings Volume 7490, PIAGENG 2009: Intelligent Information, Control, and Communication Technology for Agricultural Engineering, 749006. [2009-07-10]. International Conference on Photonics and Image in Agriculture Engineering (PIAGENG 2009), Zhangjiajie, China.

Batra N, Islam S, Venturini V, et al. 2006. Estimation and comparison of evapotranspiration from MODIS and AVHRR sensors for clear sky days over the Southern Great Plains. Remote Sensing of Environment, 103(1): 1–15.

Beguería S, Vicenteserrano S M, Angulomartínez M. 2010. A multiscalar global drought dataset: the SPEIbase: a new gridded product for the analysis of drought variability and impacts. Bulletin of the American Meteorological Society, 91(10): 1351–1356.

Beguería S, Vicenteserrano S M, Reig F, et al. 2014. Standardized precipitation evapotranspiration index (SPEI) revisited: parameter fitting, evapotranspiration models, tools, datasets and drought monitoring. International Journal of Climatology, 34(10): 3001–3023.

Cao S X. 2011. Impact of China's large-scale ecological restoration program on the environment and society in arid and semiarid areas of China: achievements, problems, synthesis, and applications. Critical Reviews in Environmental Science and Technology, 41(4): 317–335.

Cao S X, Chen L, Shankman D, et al. 2011. Excessive reliance on afforestation in China's arid and semi-arid regions: Lessons in ecological restoration. Earth-Science Reviews, 104(4): 240–245.

Dorigo W, de Jeu R, Chung D, et al. 2012. Evaluating global trends (1988–2010) in harmonized multi-satellite surface soil moisture. Geophysical Research Letter, 39(18): 18405.

Feng X M, Fu B J, Piao S L, et al. 2016. Revegetation in China's Loess Plateau is approaching sustainable water resource limits.

Nature Climate Change, 6(11): 1019–1022.

Forzieri G, Alkama R, Miralles D G, et al. 2017. Satellites reveal contrasting responses of regional climate to the widespread greening of Earth. Science, 356(6343): 1180–1184.

Ge Q S, Wang H J, Rutishauser T, et al. 2015. Phenological response to climate change in China: a meta-analysis. Global Change Biology, 21(1): 265–274.

Gong Z, Kawamura K, Ishikawa N, et al. 2015. MODIS normalized difference vegetation index (NDVI) and vegetation phenology dynamics in the Inner Mongolia grassland. Solid Earth, 6(3): 1185–1194.

He B, Chen A F, Jiang W G, et al. 2017. The response of vegetation growth to shifts in trend of temperature in China. Journal of Geographical Sciences, 27(7): 801–816.

Hu Y L, Zeng D H, Fan Z P, et al. 2008. Changes in ecosystem carbon stocks following grassland afforestation of semiarid sandy soil in the southeastern Keerqin Sandy Lands, China. Journal of Arid Environments, 72(12): 2193–2200.

Hutchinson M F. 1995. Interpolating mean rainfall using thin plate smoothing splines. International Journal of Geographical Information Systems, 9(4): 385–403.

Jiang B, Liang S L, Yuan W P. 2015. Observational evidence for impacts of vegetation change on local surface climate over northern China using the Granger causality test. Journal of Geophysical Research Biogeosciences, 120(1): 1–12.

Li X S, Wang H Y, Wang J Y, et al. 2015. Land degradation dynamic in the first decade of twenty-first century in the Beijing–Tianjin dust and sandstorm source region. Environmental Earth Sciences, 74(5): 4317–4325.

Li Y, Zhao M S, Motesharrei S, et al. 2015. Local cooling and warming effects of forests based on satellite observations. Nature Communications, 6: 6603.

Liu J H, Wu J J, Wu Z T, et al. 2013. Response of NDVI dynamics to precipitation in the Beijing–Tianjin sandstorm source region. International Journal of Remote Sensing, 34(15): 5331–5350.

Liu J Y, Kuang W H, Zhang Z X, et al. 2014. Spatiotemporal characteristics, patterns, and causes of land-use changes in China since the late 1980s. Journal of Geographical Sciences, 24(2): 195–210.

Liu X P, Zhang W J, Cao J S, et al. 2013. Carbon storages in plantation ecosystems in sand source areas of north Beijing, China. PloS ONE, 8(12): e82208.

Liu X R, Dong Y S, Ren J Q, et al. 2010. Drivers of soil net nitrogen mineralization in the temperate grasslands in Inner Mongolia, China. Nutrient Cycling in Agroecosystems, 87(1): 59–69.

Liu Y Y, Parinussa R M, Dorigo W A, et al. 2011. Developing an improved soil moisture dataset by blending passive and active microwave satellite–based retrievals. Hydrology and Earth System Sciences, 15(2): 425–436.

Ma T, Zhou C H. 2012. Climate-associated changes in spring plant phenology in China. International Journal of Biometeorology, 56(2): 269–275.

Miao L J, Luan Y B, Luo X Z, et al. 2013. Analysis of the phenology in the Mongolian Plateau by inter-comparison of global vegetation datasets. Remote Sensing, 5(10): 5193–5208.

Mitchell J M, Dzerdzeevskü B, Flohn H, et al. 1966. Climatic change. WMO Technical Note 79 (WMO-No. 195/TP. 100). Geneva: World Meteorological Organization.

Mohammat A, Wang X H, Xu X T, et al. 2013. Drought and spring cooling induced recent decrease in vegetation growth in Inner Asia. Agricultural and Forest Meteorology, 178–179: 21–30.

Mu Q Z, Zhao M S, Running S W. 2011. Improvements to a MODIS global terrestrial evapotranspiration algorithm. Remote Sensing of Environment, 115(8): 1781–1800.

Peng S S, Chen A P, Xu L, et al. 2011. Recent change of vegetation growth trend in China. Environmental Research Letters, 6(4): 044027.

Peng S S, Piao S L, Zeng Z Z, et al. 2014. Afforestation in China cools local land surface temperature. Proceedings of the National Academy of Sciences of the United States of America, 111(8): 2915–2919.

Qin Y B, Xin Z B, Yi Y, et al. 2012. Spatiotemporal variation of sandstorm and its response to vegetation restoration in Beijing–Tianjin sandstorm source area. Transactions of the Chinese Society of Agricultural Engineering, 28: 196–204. (in Chinese)

Rishmawi K, Prince S D, Xue Y K. 2016. Vegetation responses to climate variability in the northern arid to sub-humid zones of sub-Saharan Africa. Remote Sensing, 8(11): 910, doi: 10.3390/rs8110910.

Shan N, Shi Z J, Yang X H, et al. 2015. Spatiotemporal trends of reference evapotranspiration and its driving factors in the Beijing–Tianjin Sand Source Control Project Region, China. Agricultural and Forest Meteorology, 200(15): 322–333.

Shen M G, Piao S L, Jeong S J, et al. 2015. Evaporative cooling over the Tibetan Plateau induced by vegetation growth. Proceedings of the National Academy of Sciences of the United States of America, 112(30): 9299–9304.

Swenson S, Wahr J. 2006. Post-processing removal of correlated errors in GRACE data. Geophysical Research Letters, 33(8):

L08402.

Tang Q H, Zhang X J, Tang Y. 2013. Anthropogenic impacts on mass change in North China. Geophysical Research Letters, 40(15): 3924–3928.

Tian H J, Cao C X, Chen W, et al. 2015. Response of vegetation activity dynamic to climatic change and ecological restoration programs in Inner Mongolia from 2000 to 2012. Ecological Engineering, 82(4): 276–289.

Velpuri N M, Senay G B, Singh R K, et al. 2013. A comprehensive evaluation of two MODIS evapotranspiration products over the conterminous United States: Using point and gridded FLUXNET and water balance ET. Remote Sensing of Environment, 139(4): 35–49.

Vicenteserrano S M, Beguería S, Lópezmoreno J I. 2010. A multiscalar drought index sensitive to global warming: the standardized precipitation evapotranspiration index. Journal of Climate, 23(7): 1696–1718.

Wolf S, Keenan T F, Fisher J B, et al. 2016. Warm spring reduced carbon cycle impact of the 2012 US summer drought. Proceedings of the National Academy of Science of the United States of America, 113(21): 5880–5885.

Wu J J, Zhao L, Zheng Y T, et al. 2012. Regional differences in the relationship between climatic factors, vegetation, land surface conditions, and dust weather in China's Beijing–Tianjin Sand Source Region. Natural Hazards, 62(1): 31–44.

Wu Z T, Wu J J, Liu J H, et al. 2013. Increasing terrestrial vegetation activity of ecological restoration program in the Beijing–Tianjin Sand Source Region of China. Ecological Engineering, 52(52): 37–50.

Wu Z T, Wu J J, He B, et al. 2014. Drought offset ecological restoration program-induced increase in vegetation activity in the Beijing–Tianjin Sand Source Region, China. Environmental Science & Technology, 48(20): 12108–12117.

Xu L, Myneni R B, Iii F S C, et al. 2013. Temperature and vegetation seasonality diminishment over northern lands. Nature Climate Change, 3(6): 581–586.

Yang Y T, Long D, Guan H D, et al. 2015. GRACE satellite observed hydrological controls on interannual and seasonal variability in surface greenness over mainland Australia. Journal of Geophysical Research Biogeosciences, 119(12): 2245–2260.

Yu F F, Price K P, Ellis J, et al. 2003. Response of seasonal vegetation development to climatic variations in eastern central Asia. Remote Sensing of Environment, 87(1): 42–54.

Zeng X H, Zhang W J, Cao J S, et al. 2014. Changes in soil organic carbon, nitrogen, phosphorus, and bulk density after afforestation of the "Beijing–Tianjin Sandstorm Source Control" program in China. Catena, 118: 186–194.

Zhang G L, Dong J W, Xiao X M, et al. 2012. Effectiveness of ecological restoration projects in Horqin Sandy Land, China based on SPOT-VGT NDVI data. Ecological Engineering, 38(1): 20–29.